The ISC Int'l Journal of Information Security

August 2019, Volume 11, Number 3 (pp. 39–50)

http://www.isecure-journal.org

Selected Paper at the ICCMIT'19 in Vienna, Austria

Face Recognition Based Rank Reduction SVD Approach☆

Omed Hassan Ahmed *[,1,2], Joan Lu [1], Qiang Xu [1], and Muzhir Shaban Al-Ani [2]

[1] *School of Computing and Engineering, University of Huddersfield, Huddersfield, England*

[2] *Department of information Technology, University of Human Development, Sulaymaniyah, Iraq*

ARTICLE INFO.

Keywords:
Low Rank; Singular Value Decomposition; Linear Algebra; Biometric Recognition.

Abstract

Standard face recognition algorithms that use standard feature extraction techniques always suffer from image performance degradation. Recently, singular value decomposition and low-rank matrix are applied in many applications, including pattern recognition and feature extraction. The main objective of this research is to design an efficient face recognition approach by combining many techniques to generate efficient recognition results. The implemented face recognition approach is concentrated on obtaining significant rank matrix via applying a singular value decomposition technique. Measures of dispersion are used to indicate the distribution of data. According to the applied ranks, there is an adequate reasonable rank that is important to reach via the implemented procedure. Interquartile range, mean absolute deviation, range, variance, and standard deviation are applied to select the appropriate rank. Rank 24, 12, and 6 reached an excellent 100% recognition rate with data reduction up to 2 : 1, 4 : 1 and 8 : 1 respectively. In addition, properly selecting the adequate rank matrix is achieved based on the dispersion measures. Obtained results on standard face databases verify the efficiency and effectiveness of the implemented approach.

1 Introduction

Biometric recognition of both physiological and behavioral has been an active topic for researchers because of their wide range of applications in different areas of our life [1, 2]. Among all biometrics, face recognition is the most important biometric due to its wide applications, simplicity, and high uniqueness [3, 4]. Recently, face recognition has become an important issue for their huge amount of applications, especially in security [5–7]. In comparison with other biometric techniques, such as fingerprints, retina, iris, voice or gait recognition, which generally requires the cooperation of the individual, face images can be captured directly by the cameras [8, 9]. There is a large amount of data for storage and recognition; thus, this process of data reduction and retention of active data is of great importance evidenced by the following literature [10–19].

Haar and Veltkamp (2010) constructed a morphable expression model based on multiple resolution approach. In which this model automatically selects the appropriate pose, identity, and expression to adapt the 3D facial scanning [20]. Ergin (2011) applied

☆ The ICCMIT'19 program committee effort is highly acknowledged for reviewing this paper.

* Corresponding author.

Email addresses: omed.hassan@uhd.edu.iq, j.lu@hud.ac.uk, q.xu2@hud.ac.uk, mizhir.al-ani@uhd.edu.iq

ISSN: 2008-2045

base matrices to obtain the common matrix for each face class, which represents the common properties of a given face class [21]. Çarıkçı and Özen (2012) implemented face recognition approach based on Eigenfaces. In this approach, a clean face is generated for each image, then calculated the Euclidean distances between this clean face and the stored clean faces [22]. Mostafa et al. (2013) proposed a fast facial detection features approach in which these features are detected based on both appearance and geometric information [23]. Chen et al. (2014) extended dictionary and singular value of facial recognition. In this research, the intra-class variant dictionary is adopted in a subsampling situation to represent the change between samples in both learning and testing stages [24].

Dehghan et al. (2015) applied the part of the training data for data modeling in which they used concept score to describe the event, which are characteristics of confidence representation [25]. Zheng et al. (2016) implemented a learning robust fragmented representation dictionary for facial recognition that can effectively solve the occlusion problems during facial recognition [26]. Gao et al. (2017) proposed a new method by simultaneously exploiting the low range of the representation of the data and each error image induced by the occlusion, thanks to which the captured general structure of the data and the error images [27]. Wu and Ding (2018) solved the problem of face recognition using a hierarchical model based on gradients Adaptive Sparse and Low-Rank [28]. Jing et al. (2019) presented a new method to learn the discriminant representation of the tensor to implement the image classification task in a good way. [29].

In light of the above, this research proposed an efficient method to keep a minimum amount of data required for face recognition. The proposed approach aims to hybridize both singular value decomposition and dispersion measures in order to select an adequate rank of the matrix.

As an overview, there are many published works in this field which studied different approach to achieve their goals. The proposed approach aims to hybridize both singular value decomposition and dispersion measures to select an adequate rank to obtain a good result for face recognition.

2 Singular Value Decomposition

The method of matrix factorization or partition is named as Singular Value Decomposition (SVD) which is used in various applications. SVD recently has become very important and powerful tool according to high advanced in recent science and technology. SVD is an important issue in geometric linear algebra. Matrix factorization is a representation of a matrix into a product of matrices.

Let us have a matrix A with size $m*n$, so the SVD of this matrix can be factorized into the following [30]:

$$A = USV^T \tag{1}$$

where, U is a $m \times m$ orthogonal unitary matrix, S is a $m \times n$ real singular value diagonal matrix, V^T is the conjugate transpose of the n × n orthogonal unitary matrix, considering the singular values as the square root of the eigenvalues. On the other hand, this means the decomposition leading to a rotation matrix, a stretching matrix, and other rotation matrices.

Equation 1 can be represented via three geometrical transformations: rotation, resizing, and another rotation, these transformations leading to powerful properties. There is a powerful relation between Principal Component Analysis (PCA) and Singular Value Decomposition. Let us starts from the covariance matrix of A in equation 1, which can be written as [31]:

$$C = \frac{A * A}{m - 1} \tag{2}$$

Equation 2 is true only A is a centered matrix The singular vectors V in equation 1 are principal directions, so multiplying matrix A by singular values V leads to the principal components AV that given by the following equation [32]:

$$AV = USV^TV \tag{3}$$

then

$$AV = US \tag{4}$$

In order to reduce the size of data, let us map the data from m to k where $k < m$. Therefore, equation 1 can be rewritten as below [33]:

$$a_{ij} = \sum_{k=1}^{n} u_{ik}\ s_k\ v_{ik} \tag{5}$$

Equation 5 decides the number of singular values to generate. These mapping the diagonal matrix S into a vector and the variables s_i are singular values sorted from large to small value, as below [34]:

$$S_{i+1} < S_i \tag{6}$$

Matrices U and V are orthogonal, so [35],

$$UU_T = VV_T = I \tag{7}$$

where I is an identity matrix.

Using this method, we can define small singular value decomposition.

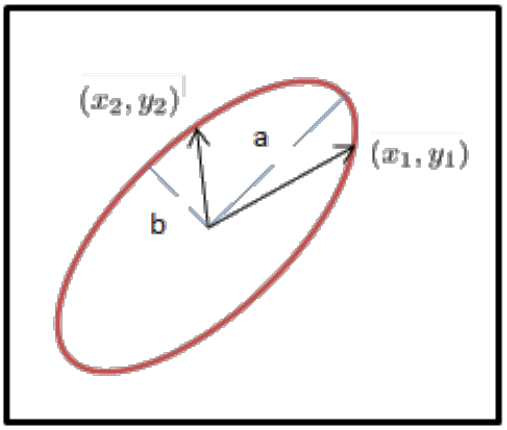

Figure 1. Ellipse Representation

Applying the orthogonal property on equation 1 to generate the following two equations [36]:

$$AA^T U = US^2 \tag{8}$$

$$AA^T V = VS^2 \tag{9}$$

From equation 8 and 9 U can be found by the projection of A into V as below [37]:

$$U = AVS^{-1} \tag{10}$$

By transposing A, U and V are changed their places as below [38]:

$$A^T = VSU^T \tag{11}$$

To realize the idea of stretching and rotating, given a two-dimensional matrix (image) in which $X_1 = (x_1, y_1)$ and $X_2 = (x_2, y_2)$, so it is possible to generate an ellipse with longer axis (a) and shorter axis (b), these can be represented by X_1 and X_2 as shown in figure 1. Let the transformed coordinates be $X^{'} = (x^{'}, y^{'})$, so we have the following [39]:

$$x = xRAM^{-1} \tag{12}$$

where,

- R is the rotation matrix and it can be written as below [40]

$$R = \begin{pmatrix} \cos(\phi) & \sin(\phi) \\ -\sin(\phi) & \cos(\phi) \end{pmatrix}$$

- M is the oriented diagonal matrix as below [41]:

$$M = \begin{pmatrix} a & 0 \\ 0 & b \end{pmatrix}$$

Therefore, the general case can be written as below [42]

$$x'_j = \frac{1}{m_j} \sum_i x_i r_{ij} \tag{13}$$

where m_j is the jth diagonal m matrix.

Thus x' and y' are given below [43]:

$$x' = \frac{x\cos(\phi) - y\sin(\phi)}{a} \tag{14}$$

$$y' = \frac{x\sin(\phi) + y\cos(\phi)}{b} \tag{15}$$

The ellipse is generated with counterclockwise direction. Turning to equation 5, in which singular value decomposition can be used to exclude the least significant components of A and only includes the most significant components. SVD for equation 1 can be modified to solve the linear equation system [44]:

$$Ax = b \tag{16}$$

$$x = VS^{-1}U^T b \tag{17}$$

Also, it can be written in another form as below [45, 46]:

$$x_i = \sum_j \frac{v_{ij}}{s_j} \sum_k u_{kj} b_k \tag{18}$$

For non-square matrix, it can be generalized the solution of normal matrix as below [30, 47]:

$$A^T Ax = A^T b \tag{19}$$

For minimum length solution of x, it is reach to origin such as below [48, 49], this generalized the linear fitting technique:

$$\min_x \; Ax - b \tag{20}$$

3 Statement of the Problem

Many algorithms are implemented for face recognition, and most of them are concentrated on the recognition rate only, yet some of these algorithms are reached a good accuracy. The proposed approach offers an efficient face recognition algorithm with a high recognition rate and minimum data size.

4 Methods Employed

Theoretic models will be employed into this investigation; then, a framework 1 will be designed to implement the models. Finally, experiments will be conducted to evaluate the developed methods.

5 Dispersion Measures

In this research, in addition to the selection of the effective rank matrix, some of the effective dispersion measures are used in recognition.

Interquartile range (irq): measures the difference between 75th and 25th percentile of the processed data.

Given:

- First quartile Q_1 = median of the n smallest entries
- Third quartile Q_3 = median of the n largest entries

interquartile range is calculated as below

$$irq = Q_3 - Q_1 \tag{21}$$

Mean absolute deviation (mad): measures the mean of distances of each value from the overall mean; it is sensitive to outliers. Let Îij be mean and N be the number of data values, so for any value x, the mean absolute deviation is given by:

$$mad = \frac{\sum|x - \mu|}{N} \tag{22}$$

Range: measures the difference between maximum and minimum values of the processed data, which indicates the simplest measure of spread.

$$Range = V_{max} - V_{min} \tag{23}$$

Variance (var): measures the average squared difference of scores from the mean score of the processed data. Variance is given by:

$$\sigma^2 = \frac{1}{N}\sum_{i=1}^{N}(x_i - \mu)^2 \tag{24}$$

Standard deviation (std): measures the square root of variance and has the desirable property of the processed data. Standard deviation is given by:

$$\sigma = \sqrt{\frac{1}{N}\sum_{i=1}^{N}(x_i - \mu)^2} \tag{25}$$

6 Design of Framework

The proposed approach comprises image acquisition, preprocessing, singular value decomposition, discrete wavelet transform and minimizing the significant number of values (figure 2).

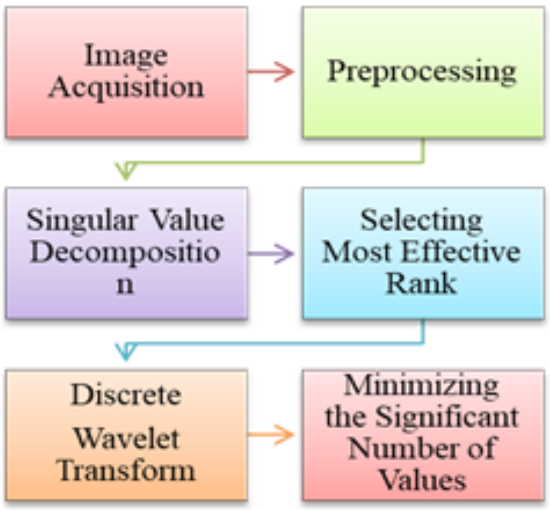

Figure 2. Designed Framework for the Investigation

- Image acquisition: in this step, ORL image data set is used to provide the face images with different positions.
- Preprocessing: in this step, many operations are implemented, such as cleaning, resizing, and filtering. Moreover, the low pass filter is applied in this step to remove the redundant noise.
- Singular value decomposition: in this step, the original image is decomposed into three orthogonal matrices, and it can be performed as rotating and stretching. Let us have a matrix A with size $m * n$ so the SVD of this matrix can be factorized into three matrices as shown in equation 1.
- Selecting the most effective rank: in this step, the measurement of dispersion in which indicated the most effective matrix rank is applied. The effective rank selection based on the degradation and similarity index via the implementation of the steps (in this case, rank 6 face matrix and rank 3 face matrix).
- The discrete wavelet transform (DWT): in this step, the discrete wavelet transform is applied to the diagonal matrix to generate effective significant features. DWT is applied via the convolution process of both low pass filter and high pass filter masks with the SVD signal.

$$y(n) = \sum_{k=0}^{N-1} s(k)\ h(2n-k)$$

- Minimizing the significant number of values: in this step, the obtained features are minimized and resized to generate a minimum number of effective values based on a certain threshold. The threshold is sited regarding the reasonable image quality based on the dispersion measures.

7 Experiments

7.1 Dataset Preparation

In this research ORL database of face images with width= 92 pixels and high= 112 pixels are used (figure 1). Different rank of face images are applied, such as: full rank face (number of columns= 46), rank 46 face (number of columns= 46), rank 24 face (number of columns= 24), rank 12 face (number of columns= 12), rank 6 face (number of columns= 6) and rank 3 (number of columns= 3). This face image dataset (ORL) comprises of Joint Photographic Experts Group (JPG or JPEG) format image and contains a set of face images of 400 grayscale face images, which are ten different images of 40 distinct persons. Each image with space size of 2.22 kB and the image dimension is $92 * 112$ (width= 92 pixels and high= 112 pixels). Some of these face images are shown in figure 3.

Figure 3. Face Image Dataset

The used face images are denoted as Face_{ij} in which the variable (i) indicates the score of the person and the variable (j) indicates the face score, this means the face image Face_{12} indicates the second face image of the first person and so on. The original face images are of size $92 * 112$; these face images are resized $2:1$, the resized images are of size $46 * 56$.

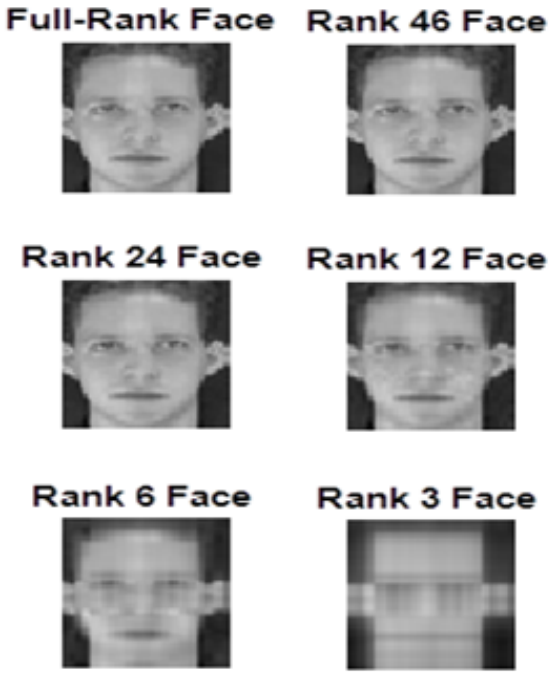

Figure 4. Faces of Different Ranks (First Person)

7.2 Results and Discussion

The standard PC has been used in the experiments by applying the Matlab simulator tool version 2015. Figure 4 shows the first face image of the first person with different ranks. The full rank face matrix and the rank 46 face matrix are the two matrices with rank equal to 46. The rank 24 face matrix has a rank of 24, the rank 12 face matrix has a rank of 12, the rank 6 face matrix has a rank of 6, and the rank 3 face matrix has a rank of 3. From this figure, it is clear that the degradation and the distortion have appeared in the last two ranks (rank 6 and 3 face matrix). In addition, the last two histograms of Figure 5 indicated a significant difference compared with the other four histograms. Image quality is measured via similarity index which has the following values according to the six rank values 1.000, 1.000, 0.9920, 0.9391, 0.8252, and 0.6682. It is clear that the first four values indicate a high-quality image, on the other hand, the last two values $(0.8252 and 0.6682)$ leading to low image quality. The sorted singular value of the first person is shown in Figure 6, these values ranged from -2.2 to 1.45. Also, the negative values started from the sixth score. The cumulative percentage of total sigma is shown in Figure 7 in which the normalized values ranged from 0.6 to 1.

It is clear that the degradation and the distortion are also appeared in the last two ranks (rank 6 face matrix and rank 3 face matrix) as shown in figure 8. In addition, the last two histograms of Figure 9

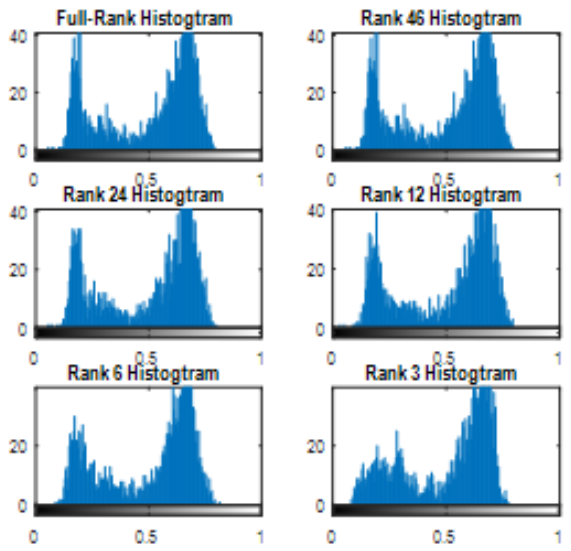

Figure 5. Histogram of Different Ranks Faces as in Figure 4 (First Person)

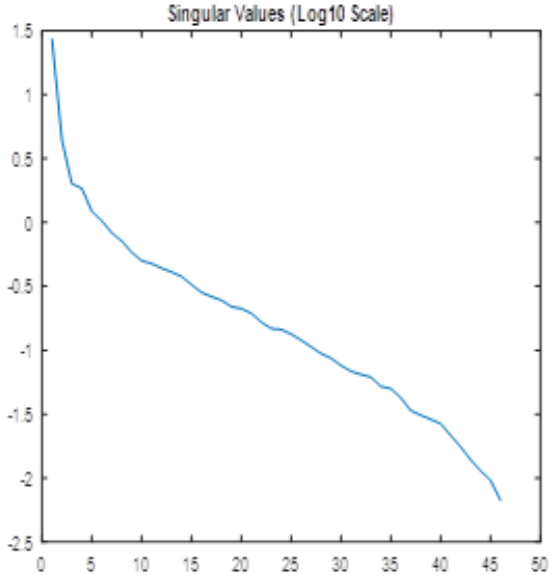

Figure 6. Sorted Singular Values (First Person)

indicated a significant difference compared with the other four histograms. Image quality is measured via similarity index which has the following values according to the six rank values 1.000, 1.000, 0.9823, 0.9000, 0.7546 and 0.5692. It is clear that the first four values indicate a high-quality image, on the other hand, the last two values (0.7546 and 0.5692) leading to low image quality, also, these values are slightly low. The sorted singular value of the first person is shown in figure 10, these values ranged from −1.8 to 1.45, in addition, the negative values started from the eight scores. The cumulative percentage of total

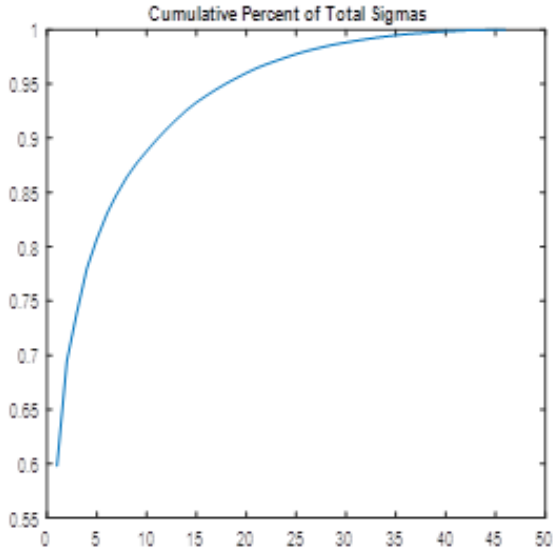

Figure 7. Cumulative Percentage of Total Sigma (First Person)

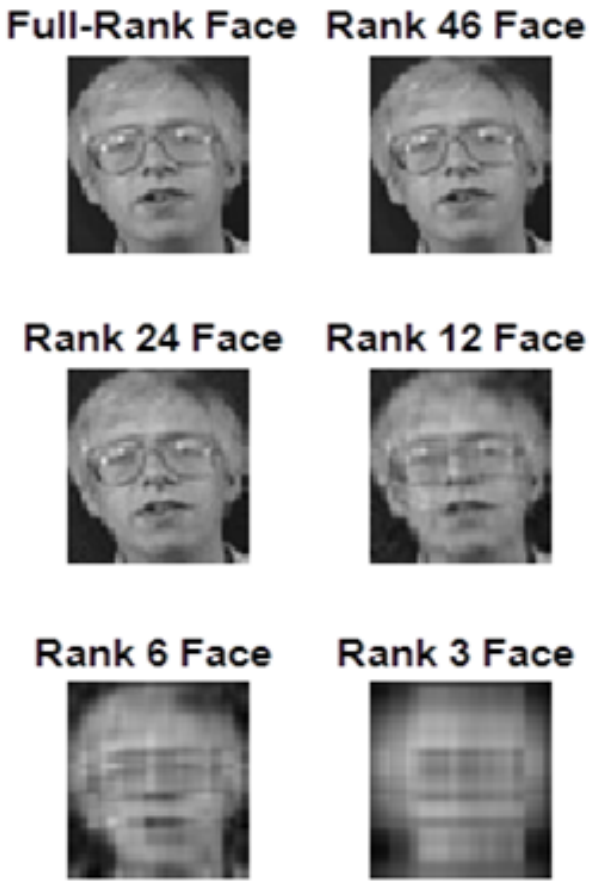

Figure 8. Faces of Different Ranks (Second Person)

sigma is shown in figure 11 in which the normalized values ranged from 0.5 to 1.

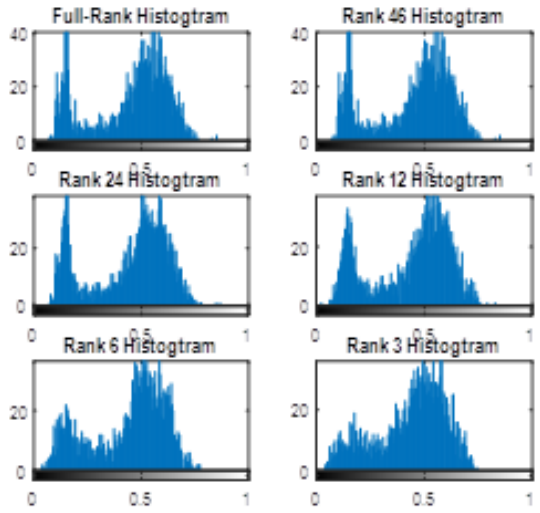

Figure 9. Histogram of Different Ranks Faces as in Figure 8 (Second Person)

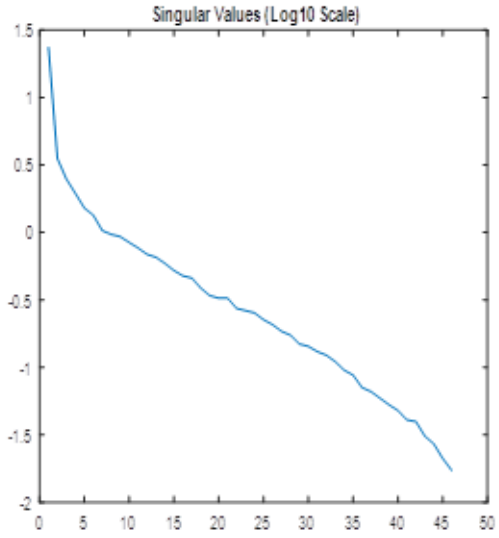

Figure 10. Sorted Singular Values (Second Person)

7.3 Measures of Dispersion Discussion

Measures of dispersion are applied to compare the first five sets of face images from the ORAL database. 50 face image of five sets of face images are compared according to their ranks. Measures of dispersion (statistical measures) are used to indicate the distribution of data.

Interquartile ranges are measured for these 50 images with different ranks (full, 46, 24, 12, 6 and 3) as shown in figure 12a. Values of interquartile ranges are used as a threshold value to indicate the adequate rank related to acceptable image quality. This research resulted that ranks full, 46 and 24 are the most acceptable set for this measurement. On the other hand, the Interquartile range values for ranks 12, 6 and 3 reached to zero.

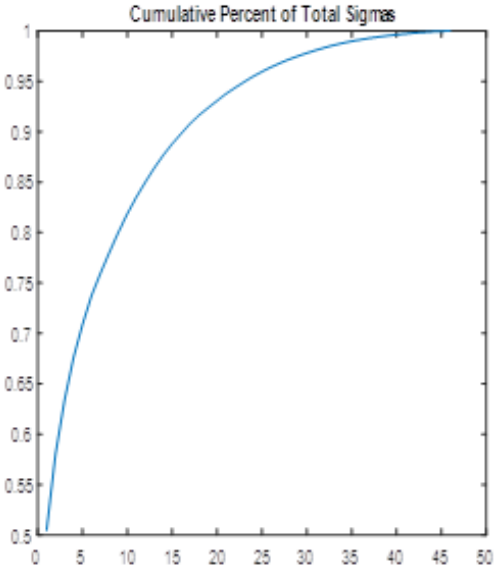

Figure 11. Cumulative Percentage of Total Sigma (Second Person)

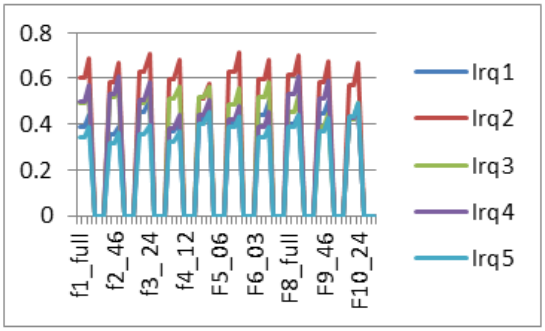

(a) Interquartile Range Values

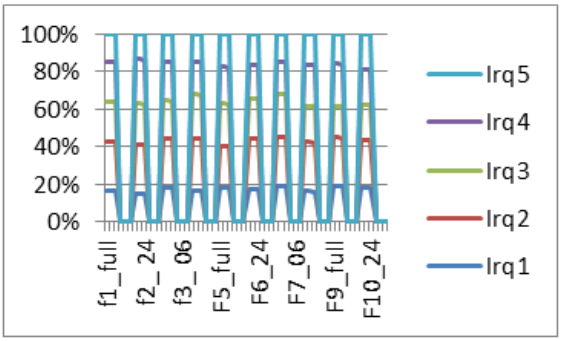

(b) Interquartile Range Percentages

Figure 12. Interquartile Ranges Measures

Mean absolute deviations are measured for these 50 images with different ranks (full, 46, 24, 12, 6 and 3) as shown in figure 12b. Mean absolute deviations

values are ranged between 1.3 and 1.5 for mad1, 1.2 and 1.3 for mad2, 1.1 and 1.3 for mad3, 1.1 and 1.4 for mad4, 1.2 and 1.3 for mad5.

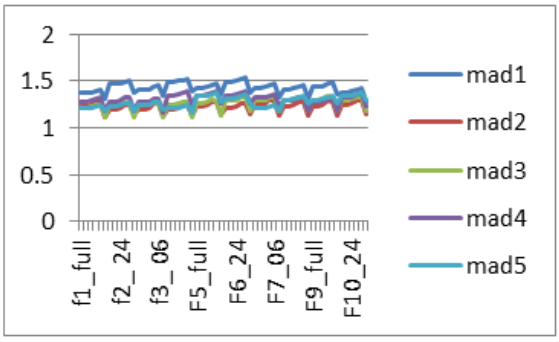

(a) Mean Absolute Deviation Values

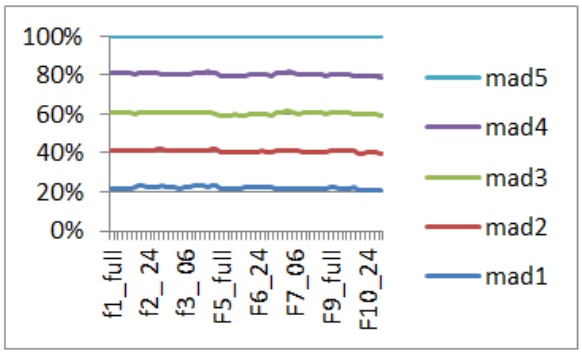

(b) Mean Absolute Deviation Percentages

Figure 13. Mean Absolute Deviation Measures

Range is measured for these 50 images with different ranks (full, 46, 24, 12, 6 and 3) as shown in figure 14. This figure shows the values of range approach to significant values for all ranks, so these ranks with range values considered to be between 27 and 30 for range1 and the obtained range values of range2 are considered to be between 23.46 and 24.16. This indicated that the obtained range values approach to similarity values between the tested faces of the same person. In addition, there is a significant difference between the range values of different persons.

Variance is measured for these 50 images with different ranks (full, 46, 24, 12, 6 and 3) as shown in figure 15. This figure shows the values of variance approach to significant values for all ranks, so these ranks with variance values considered to be between 16 and 19.85 for var1 and the obtained variance values of var2 are considered to be between 11.93 and 12.96. This indicated that the obtained variance values approach to similarity values between the tested faces of the same person. In addition, there is a significant difference between the variance values of different persons.

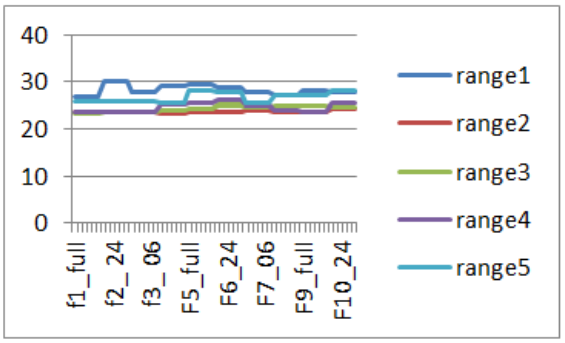

(a) Range values

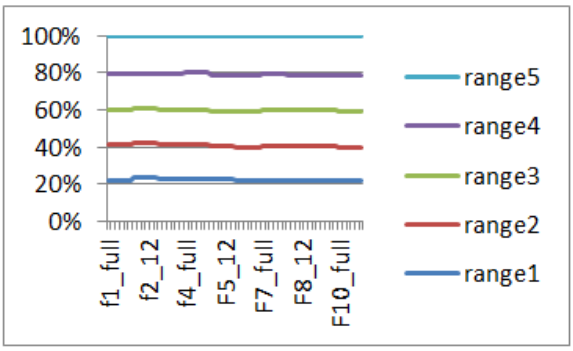

(b) Range Percentages

Figure 14. Range Measures

Standard deviation is measured for these 50 images with different ranks (full, 46, 24, 12, 6 and 3) as shown in figure 16. This figure shows the values of standard deviation approach to significant values for all ranks, so these ranks with standard deviation values considered to be between 4 and 4.42 for std1 and the obtained standard deviation values of std2 are considered to be between 3.45 and 3.55. This indicated that the obtained standard deviation values approach to similarity values between the tested faces of the same person. In addition, there is a significant difference between the standard deviation values of different persons.

8 Conclusions

8.1 Achievements

Face recognition is an important issue among biometric recognition for its simplicity and high security. Hybridizing many techniques in recognition leads to generate an efficient, high-performance approach. Low-rank matrix and SVD are used in many application of one and two-dimensional signal processing. The implemented approach consists of multi-steps, starting from preparing the face samples up to reaching a suitable rank. The implemented approach offers an efficient face recognition algorithm complaining SVD, measures of dispersion and selecting the ap-

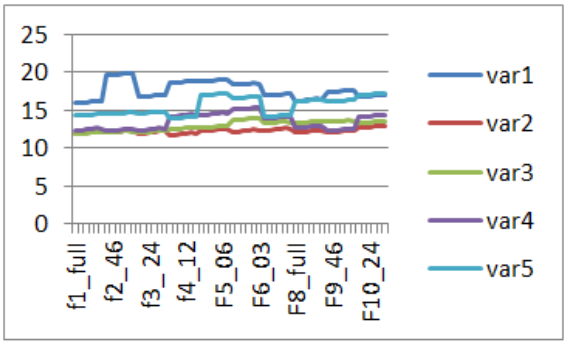

(a) Variance Values

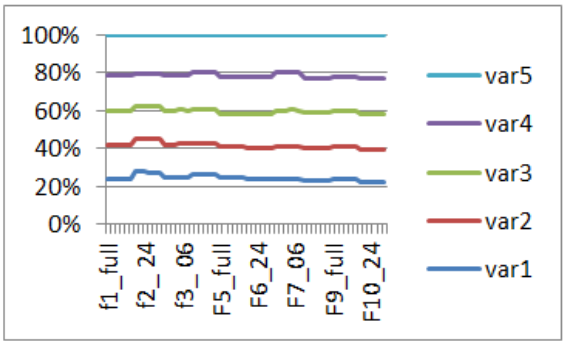

(b) Variance percentages

Figure 15. Variance measures

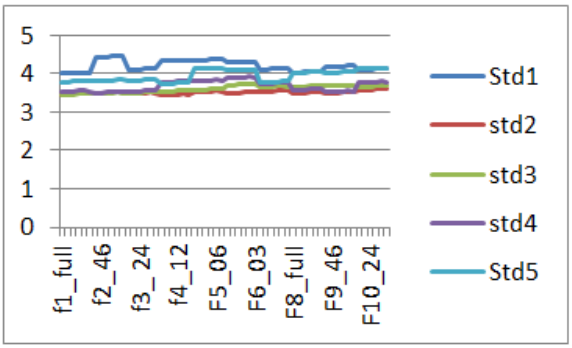

(a) Standard Deviation Values

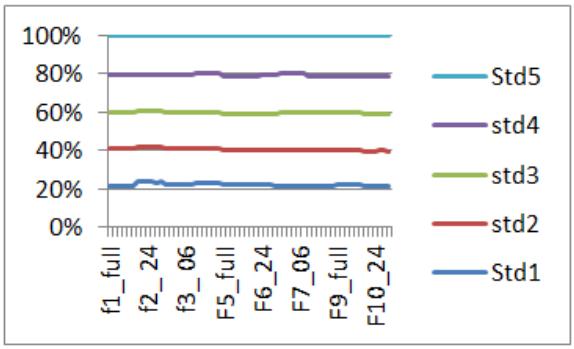

(b) Standard Deviation Percentages

Figure 16. Standard Deviation Measures

propriate rank matrix. Measures of dispersion are applied to compare the sets of face images according to their ranks. Full rank, rank 46, rank 24, rank 12, rank 6, and rank 3 are used in this research in order to reach high-performance results. The objective of this research was achieved by properly selecting the adequate rank matrix via the threshold of the dispersion measures. The research results indicated that the recognition rate of 100% is obtained within data reduction up to 8:1. Comparing with the previous works, most of these works reached a good accuracy of recognition rate, but this approach achieved a recognition rate of 100%, in addition to a high reduction in data size reached to 8 : 1.

8.2 Future Work

The implemented approach achieved acceptable results for the tested face dataset. The future work concentrated on applying this approach for different face datasets having different images sizes. In addition, as an expected proposal for future work we suggest to realize this approach as a hardware implementation to evaluate the real-time face recognition process.

References

[1] Gurjit Singh Walia, Tarandeep Singh, Kuldeep Singh, and Neelam Verma. Robust multimodal biometric system based on optimal score level fusion model. *Expert Systems with Applications*, 116:364–376, 2019.

[2] Ahmed Mahfouz, Tarek M Mahmoud, and Ahmed Sharaf Eldin. A survey on behavioral biometric authentication on smartphones. *Journal of information security and applications*, 37:28–37, 2017.

[3] Ajita Rattani and Reza Derakhshani. A survey of mobile face biometrics. *Computers & Electrical Engineering*, 72:39–52, 2018.

[4] Pedro Tome, Ruben Vera-Rodriguez, Julian Fierrez, and Javier Ortega-Garcia. Facial soft biometric features for forensic face recognition. *Forensic science international*, 257:271–284, 2015.

[5] Abdullah Mohammad Awad and Muzhir Shaban AL-Ani. An efficient approach for image hiding using hybrid technique. *Journal of Theoretical & Applied Information Technology*, 96(11), 2018.

[6] Zhiming Liu and Chengjun Liu. Fusion of color, local spatial and global frequency information for face recognition. *Pattern Recognition*, 43(8):2882–2890, 2010.

[7] R Satya Prasad, Muzhir Shaban Al-Ani, and Salwa Mohammed Nejres. An efficient approach for fingerprint recognition. *Image*, 4(5), 2015.

[8] Alaa Hussein Al-Hamami. *Handbook of Research on Threat Detection and Countermeasures in Network Security*. IGI Global, 2014.

[9] Haifeng Hu. Variable lighting face recognition using discrete wavelet transform. *Pattern Recognition Letters*, 32(13):1526–1534, 2011.

[10] Guangwei Gao, Zangyi Hu, Pu Huang, Meng Yang, Quan Zhou, Songsong Wu, and Dong Yue. Robust low-resolution face recognition via low-rank representation and locality-constrained regression. *Computers & Electrical Engineering*, 70:968–977, 2018.

[11] Nan Zhang, Yi Chen, Maolong Xi, Fangqin Wang, and Yanwen Qu. Feature extraction based on low-rank affinity matrix for biological recognition. *Journal of computational science*, 27:199–205, 2018.

[12] Baiyu Chen, Zi Yang, and Zhouwang Yang. An algorithm for low-rank matrix factorization and its applications. *Neurocomputing*, 275:1012–1020, 2018.

[13] Jicong Fan and Tommy W.S. Chow. Matrix completion by least-square, low-rank, and sparse self-representations. *Pattern Recognition*, 71:290 – 305, 2017.

[14] Hengmin Zhang, Jian Yang, Jianchun Xie, Jianjun Qian, and Bob Zhang. Weighted sparse coding regularized nonconvex matrix regression for robust face recognition. *Information Sciences*, 394:1–17, 2017.

[15] Lunke Fei, Yong Xu, Bob Zhang, Xiaozhao Fang, and Jie Wen. Low-rank representation integrated with principal line distance for contactless palmprint recognition. *Neurocomputing*, 218:264–275, 2016.

[16] LiÅčÄČ, LÄČcrÄČmioara, and Elena Pelican. A low-rank tensor-based algorithm for face recognition. *Applied Mathematical Modelling*, 39(3):1266 – 1274, 2015.

[17] Jian Zhang, Jian Yang, Jianjun Qian, and Jiawei Xu. Nearest orthogonal matrix representation for face recognition. *Neurocomputing*, 151:471 – 480, 2015.

[18] Haipeng Shen and Jianhua Z. Huang. Sparse principal component analysis via regularized low rank matrix approximation. *Journal of Multivariate Analysis*, 99(6):1015 – 1034, 2008.

[19] Nojun Kwak. Feature extraction for classification problems and its application to face recognition. *Pattern Recognition*, 41(5):1701 – 1717, 2008.

[20] Frank B. ter Haar and Remco C. Veltkamp. Expression modeling for expression-invariant face recognition. *Computers & Graphics*, 34(3):231 – 241, 2010. Shape Modelling International (SMI) Conference 2010.

[21] Semih Ergin, Serdar ÃČâĂąakir, ÃČâĂŞ. Nezih Gerek, and M. Bilginer GÃČÂijlmezoÃĎÅÿlu. A new implementation of common matrix approach using third-order tensors for face recognition. *Expert Systems with Applications*, 38(4):3246 – 3251, 2011.

[22] M.ÃČÂijge ÃČâĂąarÃĎÂśkÃČÂğÃĎÂś and Figen ÃČâĂŞzen. A face recognition system based on eigenfaces method. *Procedia Technology*, 1:118 – 123, 2012. First World Conference on Innovation and Computer Sciences (INSODE 2011).

[23] Eslam Mostafa, Riad Hammoud, Asem Ali, and Aly Farag. Face recognition in low resolution thermal images. *Computer Vision and Image Understanding*, 117(12):1689 – 1694, 2013.

[24] Si-Bao Chen, Chris H.Q. Ding, and Bin Luo. Extended linear regression for undersampled face recognition. *Journal of Visual Communication and Image Representation*, 25(7):1800 – 1809, 2014.

[25] Afshin Dehghan, Omar Oreifej, and Mubarak Shah. Complex event recognition using constrained low-rank representation. *Image and Vision Computing*, 42:13 – 21, 2015.

[26] Chun-Hou Zheng, Yi-Fu Hou, and Jun Zhang. Improved sparse representation with low-rank representation for robust face recognition. *Neurocomputing*, 198:114 – 124, 2016. Advances in Neural Networks, Intelligent Control and Information Processing.

[27] Guangwei Gao, Jian Yang, Xiao-Yuan Jing, Fumin Shen, Wankou Yang, and Dong Yue. Learning robust and discriminative low-rank representations for face recognition with occlusion. *Pattern Recognition*, 66:129 – 143, 2017.

[28] Cho Ying Wu and Jian Jiun Ding. Occluded face recognition using low-rank regression with generalized gradient direction. *Pattern Recognition*, 80:256 – 268, 2018.

[29] Peiguang Jing, Yuting Su, Zhengnan Li, Jing Liu, and Liqiang Nie. Low-rank regularized tensor discriminant representation for image set classification. *Signal Processing*, 156:62 – 70, 2019.

[30] Yegang Hu, Yuping Wang, and Jicong Zhang. Low-rank matrix recovery for source imaging with magnetoencephalography. *Optics & Laser Technology*, 110:99 – 104, 2019. Special Issue: Optical Imaging for Extreme Environment.

[31] Shanhua Zhan, Jigang Wu, Na Han, Jie Wen, and Xiaozhao Fang. Unsupervised feature extraction by low-rank and sparsity preserving embedding. *Neural Networks*, 109:56 – 66, 2019.

[32] Duc-Thuan Vo and Ebrahim Bagheri. Feature-enriched matrix factorization for relation extraction. *Information Processing & Management*, 56(3):424 – 444, 2019.

[33] Qiegen Liu, Sanqian Li, Jing Xiao, and Minghui Zhang. Multi-filters guided low-rank tensor coding for image inpainting. *Signal Processing: Image Communication*, 73:70 – 83, 2019. Tensor

Image Processing.
[34] Jianchun Xie, Jian Yang, Jianjun Qian, and Lei Luo. Bi-weighted robust matrix regression for face recognition. *Neurocomputing*, 237:375 – 387, 2017.
[35] Yixin Yang, Jianqi Zhang, Delian Liu, and Xin Wu. Low-rank and sparse matrix decomposition with background position estimation for hyperspectral anomaly detection. *Infrared Physics & Technology*, 96:213 – 227, 2019.
[36] Pranay Dighe, Afsaneh Asaei, and HervÃČÂľ Bourlard. Low-rank and sparse subspace modeling of speech for dnn based acoustic modeling. *Speech Communication*, 109:34 – 45, 2019.
[37] Hengmin Zhang, Jian Yang, Jianjun Qian, and Wei Luo. Nonconvex relaxation based matrix regression for face recognition with structural noise and mixed noise. *Neurocomputing*, 269:188 – 198, 2017.
[38] Zhen Dong, Mingtao Pei, and Yunde Jia. Orthonormal dictionary learning and its application to face recognition. *Image and Vision Computing*, 51:13 – 21, 2016.
[39] Aihua Zheng, Tian Zou, Yumiao Zhao, Bo Jiang, Jin Tang, and Chenglong Li. Background subtraction with multi-scale structured low-rank and sparse factorization. *Neurocomputing*, 328:113 – 121, 2019. Chinese Conference on Computer Vision 2017.
[40] Qiang Zhang, Zhen Huo, Yi Liu, Yunhui Pan, Caifeng Shan, and Jungong Han. Salient object detection employing a local tree-structured low-rank representation and foreground consistency. *Pattern Recognition*, 92:119 – 134, 2019.
[41] Yunfang Fu, Qiuqi Ruan, Ziyan Luo, Yi Jin, Gaoyun An, and Jun Wan. Ferlrtc: 2d+3d facial expression recognition via low-rank tensor completion. *Signal Processing*, 161:74 – 88, 2019.
[42] Taisong Jin, Jun Yu, Jane You, Kun Zeng, Cuihua Li, and Zhengtao Yu. Low-rank matrix factorization with multiple hypergraph regularizer. *Pattern Recognition*, 48(3):1011 – 1022, 2015.
[43] Junhong Lin and Song Li. Convergence of projected landweber iteration for matrix rank minimization. *Applied and Computational Harmonic Analysis*, 36(2):316 – 325, 2014.
[44] Xiao Luan, Bin Fang, Linghui Liu, Weibin Yang, and Jiye Qian. Extracting sparse error of robust pca for face recognition in the presence of varying illumination and occlusion. *Pattern Recognition*, 47(2):495 – 508, 2014.
[45] Miaoyun Zhao, Licheng Jiao, Jie Feng, and Tianyu Liu. A simplified low rank and sparse graph for semi-supervised learning. *Neurocomputing*, 140:84 – 96, 2014.
[46] Wei Han, Christian Sorg, Changgang Zheng, Qinli Yang, Xiaosong Zhang, Arvid Ternblom, Cobbinah Bernard Mawuli, Lianli Gao, Cheng Luo, Dezhong Yao, Tao Li, Sugai Liang, and Junming Shao. Low-rank network signatures in the triple network separate schizophrenia and major depressive disorder. *NeuroImage: Clinical*, 22:101725, 2019.
[47] Shengxiang Gao, Zhengtao Yu, Taisong Jin, and Ming Yin. Multi-view low-rank matrix factorization using multiple manifold regularization. *Neurocomputing*, 335:143 – 152, 2019.
[48] Jinghua Wang, Jane You, Qin Li, and Yong Xu. Orthogonal discriminant vector for face recognition across pose. *Pattern Recogn.*, 45(12):4069–4079, December 2012.
[49] Binbin Pan, Jianhuang Lai, and Pong C. Yuen. Learning low-rank mercer kernels with fast-decaying spectrum. *Neurocomput.*, 74(17):3028–3035, October 2011.

Omed Hassan Ahmed is the head of Information Technology department, College of Science and Technology at the University of Human Development in northern Iraq where he has been a faculty member since 2013. He received his B.Sc. degree Information Technology at Teesside University in the United Kingdom, HND (Higher National Diploma) in Information Technology at Teesside University in the United Kingdom and MSc in Computer Science at Newcastle University in the United Kingdom. Omed is currently a PhD researcher at Huddersfield University in the United Kingdom.

Joan Lu is in the Department of Computer Science and is the research group leader of Information and System Engineering (ISE) in the Centre of High Intelligent Computing (CHIC), having previously been a team leader in the IT department of Charlesworth Group publishing company. She successfully led and completed two research projects in the area of XML database systems and document processing in collaboration with Beijing University. Both systems were deployed as part of company commercial productions.

Qiang Xu has been Senior Lecturer in Mechanical/Automotive Engineering at the School of Computing and Engineering, since June 2013. He is a specialist in computational creep damage mechanics. Previously, Dr. Xu was Senior Lecturer in Mechanical/Manufacturing Engineering in the School of Science and Engineering at Teesside University from 2006 to 2013. In this role, He supervised a number of PhD research projects and completed over 15 consultancy and grant applications. In addition, he has held academic appointments at the Swansea Institute of Higher Education and as a Research Fellow and Senior Research Fellow at the University of Huddersfield.

Muzhir Shaban Al-Ani has received Ph. D. in Computer & Communication Engineering Technology, ETSII School, Spain, Valladolid, 1994. He has more than 30 years of teaching and researching experience and has held several academic positions both inside and outside Iraq, and has supervised more than 50 masters and doctoral dissertations. On the 1st of October 2016, he joined the Department of Computer Science, College of Science and Technology, University of Human Development, Sulaymaniyah, Iraq as a professor. His research interests concentrated on many fields: digital signal and image processing, IoT and cloud computing, biometric recognition, real-time systems, MIS and BIS, speaker identification and human identification